Pergamon

Available online at www.sciencedirect.com

SCIENCE DIRECT®

Cement and Concrete Research 33 (2003) 1021–1028

CEMENT AND CONCRETE RESEARCH

# Influence of aggregates on chloride diffusion coefficient into mortar

Sabine Caré*

*Laboratoire Central des Ponts et Chaussées, F-75732 Paris, Cedex 15, France*

Received 12 April 2001; accepted 17 December 2002

**Abstract**

In order to determine the influence of aggregates on chloride ion ingress, mortar specimens were cast with different aggregate size distribution and the same aggregate volume content. One side of the specimen was in contact with alkaline solution containing sodium chloride. The process of chloride ingress is due to diffusion. The effect of the interfacial transition zone (ITZ) around aggregate and of the tortuosity due to aggregates have been taken into account for interpreting the experimental data obtained. These two competing effects have been quantified by using the theory of composite materials. It appears that the diffusion coefficient varies as a function of the ITZ volume content and of the tortuosity.

*Keywords:* Interfacial transition zone; Diffusion; Transport properties; Chloride; Mortar

## 1. Introduction

Chloride ions contained in an environment surrounding concrete can penetrate this material and induce the corrosion of embedded reinforcing steel. Thus, it is important to know the diffusion coefficient of chloride in order to predict the initiation time of corrosion. This critical time depends on the concrete cover thickness and on the diffusion coefficient of chloride in the concrete of the studied structure. As a rule, the diffusion coefficient is determined experimentally for each case. Many authors [1,2] have reported that the influence of aggregate on chloride ingress is mainly due to the presence of an interfacial transition zone (ITZ), which results from interactions between aggregate and cement paste.

The aim of this research is to estimate the value of the diffusion coefficient of a concrete only by taking into account its proportioning. This paper reports some results corresponding to a part of this research and deals with the influence of aggregate on the diffusion coefficient.

## 2. Experimental procedures

### 2.1. Test program

The main feature of this study of the influence of aggregates on chloride diffusion in concrete is that the relevant parameter is not the aggregate content, but its size, its type and, mainly, its interaction with the cement paste in order to form an ITZ between aggregate and cement paste [3].

The influence of the ITZ on the chloride penetration was investigated using non-steady-state diffusion tests, as explained in Refs. [4,5]. The determination of chloride binding capacity was also determined.

The six specimens tested were made of Portland cement (European grade CEM I, 52.5) with a specific Blaine surface area of 3200 cm$^2$/g. One specimen was a cement paste (P) and the five remaining specimens (M1C, M2C, M2M, M1F, and M2F) were mortars with three types of aggregates: the first one was a fine siliceous sand (0.315/1 mm) labeled F, the second one was a medium-sized siliceous sand (0.315/2 mm) labeled M, and the third one was a coarse siliceous sand (2/4 mm) labeled C. Fig. 1 shows the grain size distribution of these sands. The sand volume content $C_A$ was equal to 0.25 or 0.50. The water-to-cement ratio was W/C = 0.45. A superplasticizer was used to minimize air void content. Table 1 gives the proportions of the tested materials.

---

* Present address: Laboratoire de Mécanique et Technologie, ENS Cachan, 61 avenue du President Wilson, 94235 Cachan Cedex, France. Tel.: +33-1-47-40-23-37; fax: +33-1-47-40-27-85.

*E-mail address:* sabinecare@lmt.ens-cachan.fr (S. Caré).

0008-8846/03/$ – see front matter © 2003 Published by Elsevier Science Ltd.
doi:10.1016/S0008-8846(03)00009-7

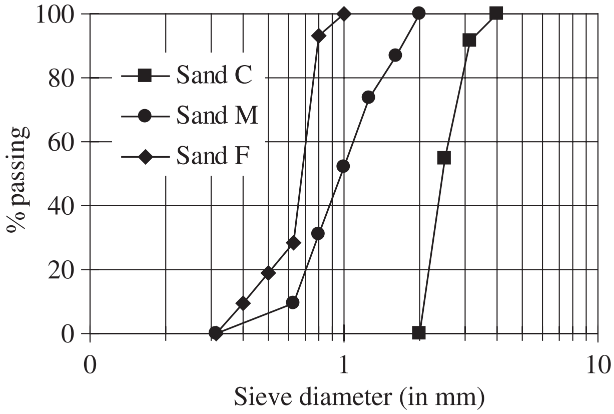

Fig. 1. Grain size distribution.

Specimens were cast in PVC cylinders 70 mm in diameter and 100 mm high. After demoulding, specimens were tightly wrapped in two superimposed adhesive aluminum sheets. Then, they were cured at 45 °C for 1 month to accelerate the hydration process and to have a "fixed" microstructure during all the experiments. After curing, the hydration degree of each material was determined by the loss of weight using the ignition method [6].

### 2.2. Microstructure analysis

The microstructure of the studied materials was investigated by Scanning Electron Microscopy (SEM) observations and by Mercury Intrusion Porosimetry (MIP) measurements.

Before testing, the samples were first frozen ( − 195 °C) by immersion into liquid nitrogen for 15 min. This quick quenching process at very low temperature allows generation of ice microcrystals that do not alter the microstructure. After freezing, samples were vacuum dried at − 55 °C for 24 h. This operation allows the ice trapped in the material porosity to sublimate. This freeze-drying technique is commonly used in many industrial areas like soil engineering, food industry, and biology. This technique is considered as a suitable procedure for MIP investigation on cement-based materials [7,8]. MIP measurements have been carried out using a CE instrument apparatus type. The instrument is capable of a minimum intruding pressure of 2.6 kPa and a maximum pressure of 200 MPa, so that the pore radius ranges from 37 Å to 60 μm. For each specimen, three samples were tested and the results averaged.

SEM is carried out using a Phillips (XL 30) microscope. Samples were impregnated with an epoxy resin, polished and then carbon coated before being observed in backscatter electron mode. As mentioned by Stutzman and Clifton [9], proper specimen preparation is necessary for an accurate study of cement-based material microstructure. Our preparation procedure was reproducible: the specimen surface was first smoothed by grinding using abrasive papers, then was polished with a diamond grid of several steps. Diamond blade slabs were lubricated using alcohol.

### 2.3. Diffusion tests

#### 2.3.1. Definition of the effective diffusion coefficient

When inside the pore system of concrete, chloride ions are partitioned between free chloride ions that diffuse toward regions with lower chloride concentration and bound chloride. The total content of chlorides by volume of porous media (kg/m$^3$), $M_{CT}$, is the sum of free and bound chlorides and is given in Eq. (1):

$$M_{CT} = M_{CB} + \Phi C_{CF} \tag{1}$$

where $M_{CB}$ is the content by volume of bound chlorides (kg/m$^3$), $C_{CF}$ is the concentration of free chloride ions in the pore solution (kg/m$^3$), and $\Phi$ is the porosity of the material.

The binding capacity of chloride $k_d$ may be defined by Eq. (2):

$$k_d = \frac{\partial m_{CB}}{\partial C_{CF}} = \frac{\partial (M_{CB}\rho_s)}{\partial C_{CF}} \tag{2}$$

where $m_{CB}$ is the weight of bound chlorides by weight of dry sample (kg/kg) and is given by $M_{CB} = \rho_s m_{CB}$ with $\rho_s$ as the dry sample specific weight (kg/m$^3$). If we assume an instantaneous exchange driven by a linear binding isotherm, $k_d$ is a constant named $K_d$.

The effective chloride diffusion coefficient $D^{\text{eff}}$ (m$^2$/s) is obtained from the steady-state regime according to the Fick's first law in Eq. (3):

$$\vec{j} = -D^{\text{eff}}\,\overrightarrow{\text{grad } C_{CF}} \tag{3}$$

where $\vec{j}$ represents the flux vector of chlorides (kg/m$^2$/s$^1$) per unit cross-sectional area.

Chloride transport in porous media is governed by Fick's second law in Eq. (4), too:

$$\frac{\partial(\Phi C_{CF})}{\partial t} = -\text{div}(-D^{\text{eff}}\,\overrightarrow{\text{grad } C_{CF}}) - \rho_s\left(\frac{\partial C_{CF}}{\partial t}k_d\right) \tag{4}$$

Because of interactions between chloride and hydrated cement paste, the chloride binding capacity has to be considered in Fick's second law.

Table 1
Proportions of materials tested

| Material | P | M1C | M2C | M2M | M1F | M2F |
|---|---|---|---|---|---|---|
| W/C | 0.45 | 0.45 | 0.45 | 0.45 | 0.45 | 0.45 |
| Aggregate | – | C | C | M | F | F |
| $C_A$ (%) | 0 | 0.25 | 0.5 | 0.5 | 0.25 | 0.5 |

W/C is the water-to-cement ratio.
$C_A$ is the relative aggregate volume content.

The effective coefficient $D^{\mathrm{eff}}$ may be measured from steady-state diffusion tests according to Eq. (3) or from non-steady-state diffusion tests according to Eq. (4). In this latter case, the effective diffusion coefficient is determined from the binding capacity and total chloride profile of materials [4,5]. Comparison between the steady-state and the non-steady-state measurements of effective chloride diffusion coefficient shows that the non-steady-state method appears to be a quick and reliable method to evaluate the effective chloride diffusion coefficient [5].

### 2.3.2. Chloride binding capacity

The binding capacity factor is evaluated from chloride binding isotherms, which are determined according to the procedure developed by Tang and Nilsson [10]. Crushed samples are immersed into basic solutions (alkaline solution with 1 g/l NaOH + 4.65 g/l KOH) with various NaCl concentrations. The cups containing the crushed samples and the chloride solutions are sealed and stored at 21 °C for a period of 1 week. According to Tang and Nilsson [10] and Francy and François [4], only 7 days of immersion are sufficient to reach the equilibrium between the solution and the solid. At the end of the immersion period, the chloride concentration of the solution is determined by means of potentiometric titration using a silver nitrate electrode according to AFREM procedures [11]. The amount of bound chloride is given by the difference between the initial and final concentration of the solution, assuming that chloride concentration in pore water is equal to that of the solution. The amount of bound chlorides is given as a function of the free chloride concentration at equilibrium.

### 2.3.3. Diffusion tests

The specimens were first immersed in a concentrated alkaline solution of KOH (4.65 g/l) and NaOH (1 g/l) and vacuum-saturated. Then, for the diffusion test, the specimens were partially immersed in a salt solution for about 40 days; the composition of the solution was 1 g/l NaOH, 4.65 g/l KOH, and 30 g/l NaCl. Fig. 2 shows the experimental setup for the diffusion test. The top of the specimen was covered with aluminum sheet to avoid evaporation so that capillary suction is negligible. The process of chloride ingress is then only diffusion.

After immersion, the specimen was taken out of the solution and its total chloride profile was determined according to AFREM procedures [11]. The sample used for determining chloride content was a slice 1.5-mm thick and 60 mm in diameter whose center was at distance $x$ from the specimen's exposed surface. After grinding, the powder was stored in a hermetically sealed bag to avoid any carbonation phenomenon.

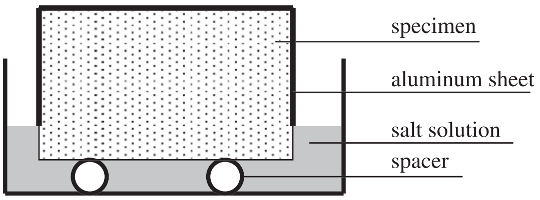

Fig. 2. Experimental setup for diffusion test. Mortar specimen is 70 mm in diameter and about 50 mm high.

Table 2
Experimental data on microstructure: hydration degree, total porosity τ, and ITZ volume content $C_{\mathrm{I}}$

| Material | P | M1C | M2C | M2M | M1F | M2F |
|---|---|---|---|---|---|---|
| Hydration degree (%) | 81.1 | 83.5 | 68.8 | 81.2 | 86.2 | 77.9 |
| Total porosity τ (%) | 22.6 | 15.1 | 11 | 12.2 | 17.9 | 13 |
| Specific surface ($m^2$/g) | 24.2 | 13.9 | 6.40 | 7.8 | 14.9 | 8.7 |
| $C_{\mathrm{I}}$ (%) | – | 1.8 | 3.6 | 10.3 | 8 | 15.4 |

## 3. Results

### 3.1. Microstructure

### 3.1.1. Hydration degree

It was important to check that cement hydration did not continue during diffusion tests. So, after curing, the hydration degree of each material was determined (Table 2). The hydration degrees of materials M1C, M2M, M1F, M2F, and P were equal to 82 ± 3%. For mortar M2C, the hydration degree, as calculated by using the value $C_{\mathrm{A}} = 0.50$, is lower than 80%. But this difference may be explained by the difficulty to cast homogeneous samples; if $C_{\mathrm{A}}$ is increased to 0.53, the hydration degree of this mortar is the same as those of the other mortars. As the hydration degree is high, the microstructure of the studied mixtures may be considered as fixed during diffusion tests.

### 3.1.2. Porosity

Fig. 3 presents the pore size distribution of the neat cement paste P and of the mortars M1C and M2C (for

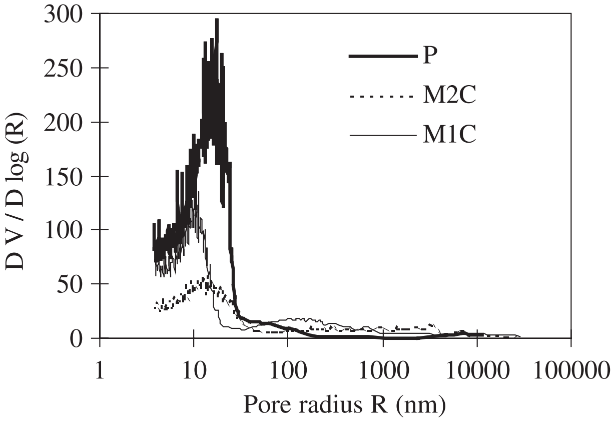

Fig. 3. Pore size distribution of the cement paste P and the mortars M1C and M2C.

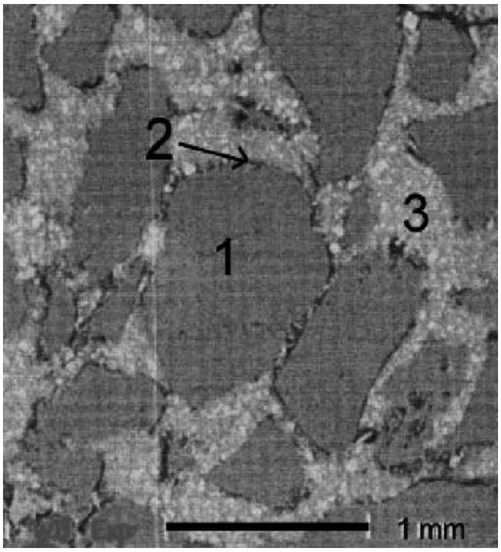

Fig. 4. SEM observations with phases 1 = aggregate, 2 = ITZ (black ring), and 3 = bulk cement paste.

other mortars, the results are identical). The presence of aggregates tends to modify the pore structure: on the one hand, the overall distributions are slightly shifted towards the finer pores and, on the other hand, coarser pores appear which may be attributed to the presence of the ITZ. The results are in accordance with previously published results [12]: more porous ITZ is expected to be accompanied by denser bulk paste (with respect to the water–cement ratio). The bulk cement paste in mortars may be all the more dense as ITZ concentration is high.

The total porosity $\tau$ for each mixture is summarized in Table 2. The total porosity of mortars is all the more high as the used sand is fine. This increase of the porosity may be associated to the ITZ volume content, which depends on the type of aggregates.

### 3.1.3. ITZ characteristics

Fig. 4 shows that aggregates were surrounded by a black ring, which characterizes the aggregate–cement ITZ. Furthermore, for the five mortars, the thickness of ITZ, $t_\mathrm{I}$, ranged from 0 to 50 μm, with a mean value around 30 μm. It does not depend on siliceous aggregate size (C, M, F) and on aggregate volume content. This ITZ thickness was equal to twice the median size of cement grains. The ITZ volume content $C_\mathrm{I}$ was, according to Garboczi and Bentz [1], given by:

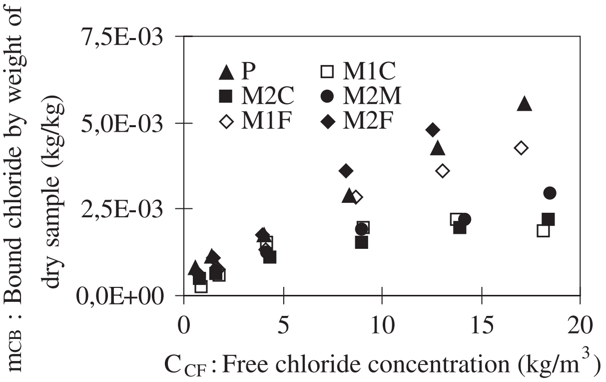

Fig. 5. Experimental results: chloride binding isothermal plots.

$$C_\mathrm{I} = 1 - e_\mathrm{V}(t_\mathrm{I}) - C_\mathrm{A} \qquad (5)$$

This equation takes into account the overlaps of the ITZs. The functional form of $e_\mathrm{V}(r)$ is given by:

$$e_\mathrm{V}(r) = (1 - C_\mathrm{A})\exp[-\pi\rho(cr + dr^2 + gr^3)] \qquad (6)$$

where ρ is the total number of aggregates per unit volume, $r$ is the thickness of a spherical shell added around each one of aggregate spherical particle, and the coefficients $c$, $d$, and $g$ are given in terms of average over the aggregate particle size distribution. The function $e_\mathrm{V}(r)$ is determined from the volume fraction of aggregates, the aggregate size distribution, which is given in Fig. 1, and the thickness of ITZ ($r = t_\mathrm{I}$). Table 2 gives the values of $C_\mathrm{I}$ for every mortar. It shows that, for a given aggregate volume content, the ITZ content $C_\mathrm{I}$ of mortars is all the higher as the used sand is fine. This means that $C_\mathrm{I}$ increases with the area of the interface between aggregate and cement.

## 3.2. Experimental results on effective diffusion coefficient

The effective diffusion coefficient is calculated from the chloride binding isotherm (Table 3 and Fig. 5) and from the total chloride profile (Fig. 6) for each mixture. From Eq. (4), the effective diffusion coefficient is given by [5]:

$$D^\mathrm{eff} = (\tau + \rho_\mathrm{s} K_\mathrm{d}) D_\mathrm{a} \qquad (7)$$

where $D_\mathrm{a}$ is the apparent diffusion coefficient, which is obtained from the total chloride profile [13,5] when the binding capacity is constant ($k_\mathrm{d} = K_\mathrm{d}$).

Table 3
Chloride binding in the tested materials

| Material | P | M1C | M2C | M2M | M1F | M2F |
|---|---|---|---|---|---|---|
| $K_\mathrm{d}$ | $2.8 \times 10^{-4}$ | $6.3 \times 10^{-5}$ | $9 \times 10^{-5}$ | $1.3 \times 10^{-4}$ | $2.3 \times 10^{-4}$ | $3.5 \times 10^{-4}$ |
| $r^2$ | .99 | .65 | .98 | .98 | .98 | .99 |

Coefficient $K_\mathrm{d}$ corresponds to the linear part of the binding isothermal curves (initial free chloride content ranging between 0.5 and 18 g/l).

Fig. 5 shows the chloride binding isothermal plots for each specimen when the initial chloride contents ranged between 0 and 20 g/l. Table 3 gives the values of binding capacity calculated between 0.5 and 18 g/l for all materials and shows that the binding capacity can be considered as constant. The value of the coefficient $K_d$ is all the more high as the ITZ concentration is high. This increase may be explained by the fact that more porous ITZ is expected to be accompanied by denser bulk cement paste, so that more chlorides are bound.

When the aggregate volume is fixed, the paste volume is fixed as well, so that the binding should be nearly constant over the different mortars. Nevertheless, with finer sand, two competing effects may be taken into account on chloride binding: the first one is due to the increase of the ITZ fraction, implying that the chloride binding is less, and the second one is due to the decrease of the bulk cement paste fraction, implying that the chloride binding increases. The second effect has to be more important because of the increase of the density of bulk cement paste. This is confirmed by the specific surface area of each mixture measured by MIP and given in Table 2.

In Fig. 6, total chloride profiles for each material are expressed vs. the Boltzmann's variable. As the test duration $t_d$ was not exactly the same for all specimens, depth $x$ was replaced by an equivalent depth. The Boltzmann's variable is $\Phi_B$, where $\Phi_B = x/\sqrt{t}$ [4].

Fig. 7 and Table 4 present the results of the effective diffusion coefficients. It has to be noticed that due to the experimental conditions, the error on the values of the effective diffusion coefficient is estimated to be about 30%. Errors on the measurements of the apparent diffusion coefficient $D_a$, the chloride binding capacity, $K_d$, and the dry sample specific weight $\rho_s$ are evaluated to be 10%. No data are available in the literature on the uncertainties on these coefficients. But the methods to determine these coefficients are reliable; thus the considered errors on these coefficients may be a good approximation. The drop in the effective diffusion coefficient between the coefficient of the cement paste P and that of the mortars M2C (and M1C) may be attributed to the presence of aggregates which induce a more tortuous path for the transport of species, as well as a phase which is much more impermeable than the cement paste.

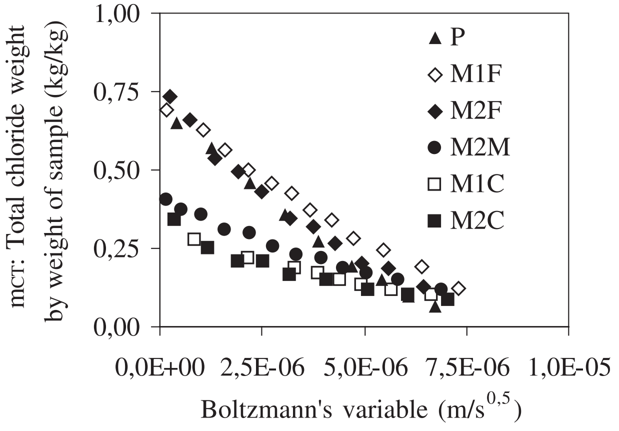

Fig. 6. Experimental results. Chloride profile: total chloride weight by weight of sample vs. Boltzmann's variable.

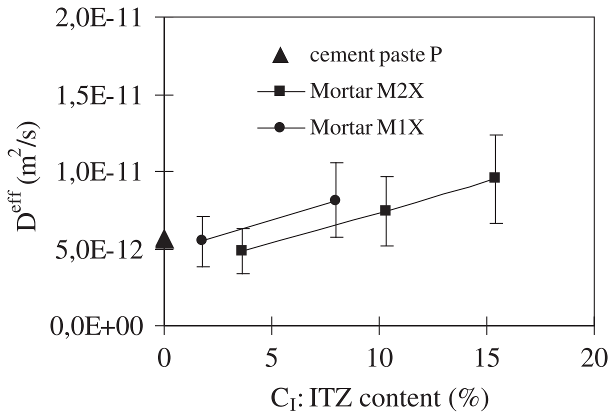

Fig. 7. Effective diffusion coefficient $D^{eff}$ vs. ITZ volume content $C_I$.

## 4. Discussion on parameters influencing diffusion coefficient

### 4.1. Effect of aggregate content

The influence of aggregate content $C_A$ on chloride diffusion coefficient is modeled by Xi and Bazant [14] according to Christensen [15]. This model assumes that, for nonporous aggregates, chloride diffusion $D^{eff}$ is:

$$D^{eff} = D_{CP} \frac{2(1 - C_A)}{2 + C_A} \tag{8}$$

where $D_{CP}$ is the effective diffusion coefficient in the cement paste.

This result is an estimation of the effective coefficient $D^{eff}$ that takes into account the cement paste–aggregate configuration in the studied materials (aggregates considered as inclusions in the cement paste). This is obtained by multiscale modeling technique.

Fig. 8 gives the values of the effective diffusion coefficient $D^{eff}$ vs. aggregate content $C_A$. For mortars where the diffusion coefficient of the cement paste $D_{CP}$ is equal to that of the paste sample P, the effective diffusion coefficient $D^{eff}$ is lower than that of the paste sample $D_{CP}$. Except for the mortars cast with the sand "C," the effective diffusion coefficient increases with the aggregate volume fraction. Thus, the model of Eq. (8) disagrees with all the experimental results. This is the reason why an improved model is needed for interpreting the data obtained.

### 4.2. Effect of ITZ concentration and of "tortuosity" T

Two parameters induced by the presence of aggregate influence chloride penetration in mortar [2]. First, diffusion

Table 4
Effective diffusion coefficients (m$^2$/s) for all materials

| Material | P | M1C | M2C | M2M | M1F | M2F |
|---|---|---|---|---|---|---|
| (1) $D^{\text{eff}}$ | $5.65 \times 10^{-12}$ | $5.4 \times 10^{-12}$ | $4.8 \times 10^{-12}$ | $7.4 \times 10^{-12}$ | $8.1 \times 10^{-12}$ | $9.5 \times 10^{-12}$ |
| (2) $D^{\text{eff}}$ from Eq. (14) | – | $4.8 \times 10^{-12}$ | $4 \times 10^{-12}$ | $7.4 \times 10^{-11}$ | $8.2 \times 10^{-11}$ | $9.9 \times 10^{-11}$ |
| Deviation (%) [(1) – (2)]/(1) × 100 | – | – 13 | – 16 | – 1 | + 1 | + 4 |

Experimental (1) and predicted values (2) from Eq. (14).

path is longer compared to plain cement paste. Second, the formation of an ITZ around aggregates in mortar increases chloride ingress. These two competing effects are taken into account as follows. Two tortuosities may be defined. The first tortuosity, *T*, is induced by the aggregates and said here to be macroscopic. The second, *t*, is the tortuosity of the pore network, said here to be microscopic.

For a porous media with porosity Φ, analytical solution for the effective diffusion coefficient is given in previous works [16,17] such as:

$$D^{\text{eff}} = D_0^{\Phi t} = D_0 \frac{2\Phi}{3 - \Phi} \tag{9}$$

where $D_0$ is the diffusion coefficient of ions in water and *t* is the tortuosity of the pore network, said here to be microscopic, of the porous media and is estimated by [17]:

$$t = \frac{2}{3 - \Phi} \tag{10}$$

These results are obtained by multiscale modeling technique using Mori Tanaka's approach [17] as an estimation of the effective diffusion coefficient from describing the solid grains as inclusions in a fluid phase. For cement-based materials, definition of tortuosity *t* means anything because solid grains as inclusions in a fluid phase cannot describe these materials. Nevertheless, in the case of nonporous aggregates, which may be considered as inclusions in the cement paste and by analogy with Eq. (9), the effective diffusion coefficient $D^{\text{eff}}$ of the medium with aggregates may be estimated by Eq. (8) where $D_{\text{CP}}$ (the diffusion coefficient of the cement paste) is used instead of $D_0$ and where the porosity τ is replaced by the volume fraction of aggregates $(1 - C_{\text{A}})$, which represents the phase where the chloride ions diffuse.

Then, the effective diffusion coefficient of concrete can be written as:

$$D^{\text{eff}} = D_{\text{CP}}(1 - C_{\text{A}})T \tag{11}$$

where the change of chloride path is described by the tortuosity parameter *T*, which is:

$$T = \frac{2}{2 + C_{\text{A}}} \tag{12}$$

The tortuosity *T* only depends on the volume fraction of aggregates and does not depend on the particle size distribution of the aggregates. This tortuosity *T*, as for the tortuosity *t*, is a function of the increase of way for diffusive species due to a tortuous path induced by aggregates, as mentioned by Delagrave et al. [2].

However, the obtained data show that, for given values of parameters $C_{\text{A}}$ and *T*, diffusion coefficients vary, depending on ITZ content $C_{\text{I}}$. So, the best model for interpreting the obtained data is as follows. The presence of aggregates influences the chloride diffusion coefficient in mortar by a geometry effect and by a local microstructure effect. The geometry effect is described by one of these two linked parameters, aggregate content $C_{\text{A}}$ and tortuosity *T*. The local microstructure effect is described by ITZ volume content $C_{\text{I}}$. Fig. 7 shows that, for a given tortuosity *T*, the relationship between $D^{\text{eff}}$ and $C_{\text{I}}$ appears linear. This relationship may be written with $D_{\text{P}}$, the diffusion coefficient of the cement paste P, without aggregate:

$$D^{\text{eff}} = D_{\text{P}}(mC_{\text{I}} + n)T \tag{13}$$

For $C_{\text{I}} = 0$, Eq. (13) is the same as Eq. (8) and $D_{\text{CP}} = D_{\text{P}}$, then *n* is equal to $(1 - C_{\text{A}})$. The value *m* is given in Fig. 9 and is estimated from experimental data by $m = 0.11C_{\text{I}}$ with a good correlation coefficient $r^2$ ($r^2$=.94). The diffusion

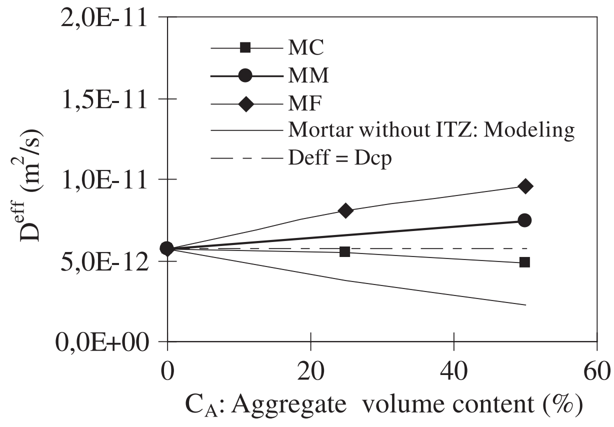

Fig. 8. Effective diffusion coefficient $D^{\text{eff}}$ vs. aggregate volume content $C_{\text{A}}$. The solid line corresponds to Eq. (8) where $D_{\text{CP}}$ is the diffusion coefficient in the cement paste P.

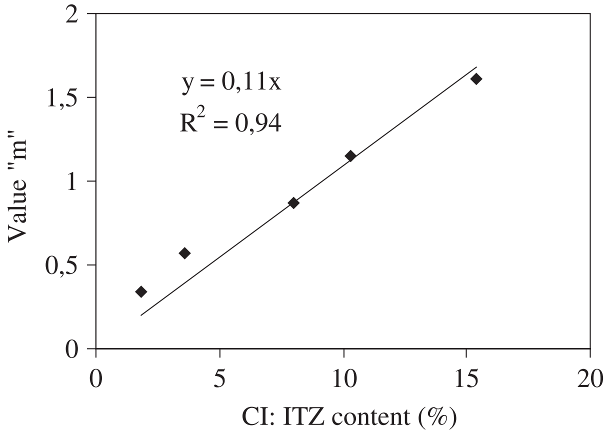

Fig. 9. Value *m* plotted vs. ITZ volume content.

coefficient $D^{\mathrm{eff}}$ for the studied materials is then estimated by:

$$D^{\mathrm{eff}} = D_{\mathrm{P}}[0.11C_{\mathrm{I}} + (1 - C_{\mathrm{A}})]\frac{2}{2 + C_{\mathrm{A}}}$$

$$D^{\mathrm{eff}} = D_{\mathrm{P}}\left[0.11C_{\mathrm{I}} + \frac{3T - 2}{T}\right]T \qquad (14)$$

This result shows that, in this case, the two effects of the aggregates on the effective diffusion coefficient can be decoupled. The effective diffusion coefficient can be expressed as a function of the ITZ content and the aggregate volume content or as a function of the ITZ content and the tortuosity *T*. If the model given in Eq. (14) is considered, the predicted values of $D^{\mathrm{eff}}$ are given in Table 4. The difference between the predicted values and the experimental coefficients is less than the experimental uncertainties. Thus, a procedure to estimate the diffusion coefficient $D^{\mathrm{eff}}$ of chloride in mortar can be as follows. When this diffusion coefficient is known for the related cement paste (without aggregate) and for a reference mortar, it can be estimated for any other mortars with any aggregate volume content and any aggregate size distribution.

## 5. Conclusions

The aim of this paper was to analyze the effect of aggregates on the effective diffusion coefficient. The test results presented in this paper indicate that the aggregates modify the pore structure of the cement paste and the transport properties. The two effects due to aggregates, ITZ content, and tortuosity *T* are quantified from multiscale modeling technique. Our results show that the effective diffusion coefficient can be given as a function of the ITZ content and the tortuosity *T*. The ITZ content depends on the volume fraction of aggregates, the aggregate size distribution, and the thickness of ITZ. The tortuosity *T* depends on the volume fraction of aggregates and does not depend on the particle size distribution of aggregates. This parameter is characterized by the increase of way for diffusive species due to a tortuous path induced by aggregates.

## Acknowledgements

J.J. Serrano and R. Leroy (LCPC) are thanked for grateful discussion for the elaboration of the experimental program. A. Raharinaivo (LCPC) is thanked for his remarks, too.

## References

[1] E.J. Garboczi, D.P. Bentz, Analytical formulas for interfacial transition zone properties, Adv. Cem. Based Mater. 6 (1997) 99–108.

[2] A. Delagrave, J.P. Bigas, J.P. Ollivier, J. Marchand, M. Pigeon, Influence of the interfacial zone on the chloride diffusivity of mortars, Adv. Cem. Based Mater. 5 (1997) 86–92.

[3] J.P. Ollivier, J.C. Maso, B. Bourdette, Interfacial transition zone in concrete, Adv. Cem. Based Mater. 2 (1995) 30–38.

[4] O. Francy, R. François, Measuring chloride diffusion coefficients from non-steady state diffusion tests, Cem. Concr. Res. 28 (1998) 947–953.

[5] R. François, O. Francy, S. Caré, V. Baroghel Bouny, P. Lovera, C. Richet, Mesure du coefficient de diffusion des ions chlorures: comparaison régime permanent-régime transitoire, Revue Française de Génie Civil 5 (2–3) (2001) 309–329.

[6] M. Mouret, A. Bascoul, G. Escadeillas, Study of the degree of hydration of concrete by means of image analysis and chemically bound water, Adv. Cem. Based Mater. 6 (1997) 109–115.

[7] C. Gallé, Effect of drying on cement-based materials pore structure as identified by mercury intrusion porosimetry. A comparative study between oven-, vacuum- and freeze-drying, Cem. Concr. Res. 31 (2001) 1467–1477.

[8] A. Kumar, D.M. Roy, The effect of desiccation on the porosity and pore structure of freeze-dried hardened Portland cement and slag-blended pastes, Cem. Concr. Res. 16 (1) (1986) 74–78.

[9] P.E. Stutzman, J.R. Clifton, Specimen preparation for scanning electron microscopy, Twenty-first International Conference on Cement Microscopy, Las Vegas, NV, 25–29 April, 1999.

[10] L. Tang, L.O. Nilsson, Chloride binding capacity and binding isothermal plots of OPC pastes and mortars, Cem. Concr. Res. 23 (1993) 247–253.

[11] T. Chaussadent, G. Arliguie, AFREM test procedures concerning chlorides in concrete: extraction and titration methods, Mat. Struct. 32 (1999) 230–234.

[12] A. Bentur, M.G. Alexander, A review of the work of the Rilem TC 159-ETC. Engineering of the interfacial transition zone in cementitious composites, Mat. Struct. 33 (2000) 82–87.

[13] E. Poulsen, The chloride diffusion characteristics of concrete—Approximative determination by linear regression analysis, Nordic Concrete Research, Publication 9, Nordic Concrete Federation, Oslo, Norway, 1990, pp. 124–133.

[14] Y. Xi, Z.P. Bazant, Modeling chloride penetration in saturated concrete, J. Mater. Civ. Eng. (February 1999) 58–65.

[15] R.M. Christensen, Mechanics of Composite Materials, Wiley-Interscience, New York, 1979.

[16] J. Van Brakel, P.M. Heetjes, Analysis of diffusion in macroporous

media in terms of a porosity, a tortuosity and a constrictivity factor, Int. J. Heat Mass Transfer 17 (1974) 1093–1103.

[17] L. Dormieux, E. Lemarchand, Modélisation macroscopique du transport diffusif, apport des méthodes de changement d'espace, Oil Gas Sci. Technol. Rev. IFP 55 (1) (2000) 15–34.

## Glossary

$C_{CF}$: concentration of free chloride ions in the pore solution (kg/m$^3$)

$C_A$: sand volume content

$C_I$: ITZ volume content

$D^{eff}$: effective chloride diffusion coefficient (m$^2$/s)

$D_a$: apparent diffusion coefficient (m$^2$/s)

$D_{CP}$: effective diffusion coefficient in the cement paste of the mortar (m$^2$/s)

$D_P$: effective diffusion coefficient in the cement paste without aggregate (m$^2$/s)

$D_o$: diffusion coefficient of chloride ions in water

$j$: flux vector of chlorides (kg/m$^2$/s per unit cross-sectional area)

$k_d$: binding capacity of chloride defined named $K_d$ if $k_d$ is a constant

$M_{CT}$: total content of chlorides by volume of porous media (kg/m$^3$)

$M_{CB}$: content of bound chlorides by volume of porous media (kg/m$^3$)

$m_{CB}$: weight of bound chlorides by weight of dry sample (kg/kg)

$t$: tortuosity of the pore network of a porous media

$T$: tortuosity due to aggregates that change chloride path

$t_I$: thickness of ITZ (mm)

$t_d$: test duration (s)

$W/C$: water-to-cement ratio

$x$: distance from the specimen exposed surface

$\Phi$: total porosity of the material

$\rho_s$: dry sample specific weight (kg/m$^3$)

$\Phi_B$: Boltzmann's variable